Bioconjugate Chemistry

Article

pubs.acs.org/bc

A Potent Anti-CD70 Antibody–Drug Conjugate Combining a Dimeric Pyrrolobenzodiazepine Drug with Site-Specific Conjugation Technology

Scott C. Jeffrey,* Patrick J. Burke,† Robert P. Lyon,† David W. Meyer,† Django Sussman,† Martha Anderson,† Joshua H. Hunter,† Chris I. Leiske,† Jamie B. Miyamoto,† Nicole D. Nicholas,† Nicole M. Okeley,† Russell J. Sanderson,† Ivan J. Stone,† Weiping Zeng,† Stephen J. Gregson,‡ Luke Masterson,‡ Arnaud C. Tiberghien,‡ Philip W. Howard,‡ David E. Thurston,§ Che-Leung Law,† and Peter D. Senter†

†Department of Research & Translational Medicine, Seattle Genetics, Inc., Bothell, Washington 98021, United States

‡Spirogen Ltd., QMB Innovation Centre, 42 New Road, London E1 2AX, United Kingdom

§Department of Pharmacy, Institute of Pharmaceutical Sciences, King's College London, Britannia House, 7 Trinity Street, London SE1 1DB

Supporting Information

ABSTRACT: A highly cytotoxic DNA cross-linking pyrrolobenzodiazepine (PBD) dimer with a valine-alanine dipeptide linker was conjugated to the anti-CD70 h1F6 mAb either through endogenous interchain cysteines or, site-specifically, through engineered cysteines at position 239 of the heavy chains. The h1F6$_{239C}$-PBD conjugation strategy proved to be superior to interchain cysteine conjugation, affording an antibody–drug conjugate (ADC) with high uniformity in drug-loading and low levels of aggregation. In vitro cytotoxicity experiments demonstrated that the h1F6$_{239C}$-PBD was potent and immunologically specific on CD70-positive renal cell carcinoma (RCC) and non-Hodgkin lymphoma (NHL) cell lines. The conjugate was resistant to drug loss in plasma and in circulation, and had a pharmacokinetic profile closely matching that of the parental h1F6$_{239C}$ antibody capped with N-ethylmaleimide (NEM). Evaluation in CD70-positive RCC and NHL mouse xenograft models showed pronounced antitumor activities at single or weekly doses as low as 0.1 mg/kg of ADC. The ADC was tolerated at 2.5 mg/kg. These results demonstrate that PBDs can be effectively used for antibody-targeted therapy.

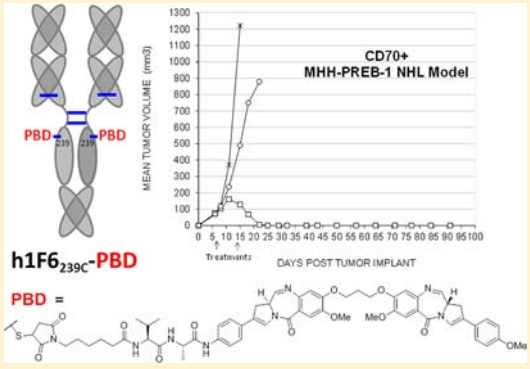

INTRODUCTION

ADCs have attracted significant interest for cancer therapy, largely based on the approved drugs ADCETRIS (brentuximab vedotin) and KADCYLA (ado-trastuzumab emtansine) for the treatment of CD30 and Her2/neu-positive malignancies, respectively.[1] Both ADCs employ antimitotic agents as the drug payload and serve as prototypes for many related agents that are in various stages of preclinical and clinical development. Currently, there are more than 20 ADCs in clinical trials spanning a variety of solid and hematologic cancer indications.[2,3]

In the effort to extend the technology and identify and optimize key parameters that lead to highly active and well-tolerated ADCs, numerous drug types,[4−7] linker strategies,[8,9] antigen targets,[2] and antibody formats[10] have been investigated. Factors such as drug potency and mechanism,[11] linker stability,[12] drug release mechanism,[9,13] conjugate composition,[14] pharmacokinetics,[10] antigen expression,[15] internalization, and distribution[16] have all been identified as important considerations for optimal ADC performance.

In this current work, we extend ADC technology to include a highly potent and broadly active PBD dimer[17,18] as a drug payload. Previously,[19] we demonstrated that a PBD-based ADC had pronounced activity in models of acute myelogenous leukemia. We extend these findings to include other malignancies and illustrate how the hydrophobic properties of the PBD dimer require site-specific conjugation to minimize aggregation caused by more highly loaded ADC species. This was achieved through a serine-to-cysteine mutation at position 239 of the h1F6 (anti-CD70) antibody heavy chains, facilitating selective drug attachment. The resulting h1F6$_{239C}$-PBD conjugate was well characterized, induced immunologically specific cell kill in vitro, and was highly active in vivo. This new

Received: April 29, 2013
Revised: June 11, 2013
Published: June 12, 2013

anticancer agent incorporates several advancements in ADC technology.

EXPERIMENTAL PROCEDURES

General Methods and Materials. Commercially available anhydrous solvents were used without further purification. Analytical thin layer chromatography was performed on silica gel 60 F254 aluminum sheets (EMD Chemicals, Gibbstown, NJ). Radial chromatography was performed on a Chromatotron apparatus (Harris Research, Palo Alto, CA). Analytical HPLC was performed on a Varian ProStar 210 solvent delivery system configured with a Varian ProStar 330 PDA detector. Samples were eluted over a C12 Phenomenex Synergi 2.0 × 150 mm, 4 μm, 80 Å reversed-phase column. The acidic mobile phase consisted of acetonitrile and water, both containing 0.1% formic acid. Compounds were eluted with a linear gradient of acidic acetonitrile from 5% at 1 min post injection, to 95% at 11 min, followed by isocratic 95% acetonitrile to 15 min (flow rate = 1.0 mL/min). LC-MS was performed on a ZMD Micromass mass spectrometer interfaced to an HP Agilent 1100 HPLC instrument equipped with a C12 Phenomenex Synergi 2.0 × 150 mm, 4 μm, 80 Å reversed-phase column. The acidic eluent consisted of a linear gradient of acetonitrile from 5% to 95% in 0.1% aqueous formic acid over 10 min, followed by isocratic 95% acetonitrile for 5 min (flow rate = 0.4 mL/min).

(*S*)-2-((*S*)-2-(6-(2,5-Dioxo-2,5-dihydro-1*H*-pyrrol-1-yl)-hexanamido)-3-methylbutanamido)propanoic acid (mc-val-ala-OH). To a solution of H_2N-Valine-Alanine-OH dipeptide (200 mg, 1.06 mmol) dissolved in anhydrous DMF (10.6 mL) was added maleimidocaproyl NHS ester (327 mg, 1.06 mmol). Diisopropylethylamine (0.92 mL, 5.3 mmol) was then added and the reaction mixture was stirred under nitrogen at ambient temperature for 18 h, at which time TLC and analytical HPLC revealed consumption of the starting materials. The reaction was diluted with 0.1 M HCl (100 mL) and the aqueous layer was extracted with ethyl acetate (3 × 100 mL). The combined organic layer was washed with water and brine, then dried over sodium sulfate, filtered, and concentrated. The crude product was dissolved in minimal dichloromethane and purified by radial chromatography on a 2 mm chromatotron plate eluted with dichloromethane/methanol mixtures (95:5 to 90:10 dichloromethane/methanol) to provide 158 mg (39%) as an white solid. TLC: Rf = 0.26, 10% methanol in dichloromethane. ^{1}H NMR (400 MHz, $CDCl_3$) (ppm) 0.95 (d, J = 17 Hz, 3H), 0.98 (d, J = 17 Hz, 3H), 1.30 (m, 2H), 1.40 (d, J = 17 Hz, 3H), 1.61 (m, 4H), 2.06 (m, 1H), 2.25 (dt, J = 4, 19 Hz, 2H), 3.35 (s, 1H), 3.49 (t, J = 17 Hz, 2H), 4.20 (d, J = 18 Hz, 1H), 4.38 (m, 1H), 6.80 (s, 2H). Analytical HPLC (0.1% formic acid): t_R 9.05 min. LC-MS: t_R 11.17 min, m/z (ES+) expected 382.2 $(M+H)^+$, found 381.9, m/z (ES-) expected 380.2 $(M-H)^-$, found 379.9.

6-(2,5-Dioxo-2,5-dihydro-1*H*-pyrrol-1-yl)-*N*-((*S*)-1-(((*S*)-1-((4-((*S*)-7-methoxy-8-(3-(((*S*)-7-methoxy-2-(4-methoxyphenyl)-5-oxo-5,11*a*-dihydro-1*H*-benzo[*e*]pyrrolo[1,2-*a*][1,4]diazepin-8-yl)oxy)propoxy)-5-oxo-5,11*a*-dihydro-1*H*-benzo[*e*]pyrrolo[1,2-*a*][1,4]diazepin-2-yl)phenyl)-amino)-1-oxopropan-2-yl)amino)-3-methyl-1-oxobutan-2-yl)hexanamide (PBD-linker). To a mixture of mc-val-ala-OH (157 mg, 0.41 mmol) in a 5% methanol/dichloromethane mixture (3 mL) was added EEDQ (102 mg, 0.41 mmol). The mixture was stirred for 30 min, followed by cooling to 0 °C and the addition of solid PBD dimer[20] (100 mg, 0.138 mmol). The ice-bath was removed and the reaction mixture was allowed to stir for 3 h. The mixture was aspirated onto a 2 mm radial chromatography plate and eluted with 3% methanol in dichloromethane. The fractions were analyzed by TLC (5% methanol/dichloromethane) and product-containing fractions were combined and concentrated to give 67 mg (45%). Analytical HPLC (0.1% formic acid): t_R 11.51 min. LC-MS: t_R 12.73 min, m/z (ES+) expected 1089.5 $(M+H)^+$, found 1089.6 m/z (ES-) expected 1087.4 $(M-H)^-$, found 1087.3.

Conjugate Preparation. The CD70 antibody engineered with a cysteine residue at position 239 of the heavy chain ($h1F6_{239C}$) was fully reduced by adding 10 equiv of TCEP and 1 mM EDTA and adjusting the pH to 7.4 with 1 M Tris buffer (pH 9.0). Following 1 h incubation at 37 °C, the reaction was cooled to 22 °C and 30 equiv of dehydroascorbic acid were added. The pH was adjusted to 6.5 with 1 M Tris buffer (pH 3.7) and the oxidation reaction was allowed to proceed for 1 h at 22 °C. This resulted in reformation of native disulfides, but left the cysteines at position 239 in the reduced state and available for conjugation. The pH of the solution was then raised again to 7.4 by addition of 1 M Tris buffer (pH 9.0). To maintain solubility of the PBD-linker, the antibody itself was diluted with propylene glycol to a final concentration of 33%. The solution of PBD linker (3.0 equiv) in propylene glycol was added to the antibody solution to effect the conjugation. The final concentration of propylene glycol in the conjugation reaction was 50%. The reaction was allowed to proceed for 30 min. The mixture was treated with activated charcoal as a slurry in propylene glycol and water for 30 min. The activated charcoal was then removed by filtering. Extent of aggregation was determined by size exclusion chromatography. Drug-loading was determined by reducing the ADC with $NaCNBH_3$ and dithiothreitol followed by HPLC analysis on a PLRP column and integration of the heavy and light chain components.

In Vitro Assays. The following cells were treated with PBD dimer and PBD ADCs: 786-O (500 cells/well), Caki-1 (1000 cells/well), UM-RC-3 (1500 cells/well), ACHN (3000 cells/well), MHH-PREB-1 and Raji (7000 cells/well), WSU-NHL (7000 cells/well), and KMH2 (2000 cells/well). The tissue culture media consisted of DMEM, 10% FBS, and 1% sodium pyruvate, nonessential amino acids, and L-glutamine (LifeTech, Carlsbad, CA). The assay was conducted in 96-well, clear flat-bottom, black-sided plates. The cells were plated (150 μL/well) one day prior to treatment, allowed to adhere in a biological safety cabinet for 1 h, then placed in a CO_2 incubator overnight. Cells were then treated with PBD dimer or ADC and incubated at 37 °C for 96 h under a 5% CO_2 atmosphere. After 96 h, the cells were labeled with Cell Titer Glo (Promega, Madison, WI, 100 μL/well) and after shaking for 2 min and incubation for an additional 25 min in the dark, luminescence was measured on a plate reader. The IC_{50} values, determined in triplicate, are defined here as the concentration that results in a 50% reduction in cell growth relative to untreated controls.

Xenograft Studies. All experiments were conducted in concordance with the Institutional Animal Care and Use Committee in a facility fully accredited by the Association for Assessment and Accreditation of Laboratory Animal Care. ACHN and Raji lymphoma disseminated models: Female C.B-17 SCID mice (n = 10, Harlan, Indianapolis, IN) were injected intraperitoneally (ip) with ACHN cells (10^6) or intravenously (iv) Raji lymphoma cells (5×10^6). The $h1F6_{239C}$-PBD and $hIgG_{239C}$-PBD ADCs were dosed ip according to schedule at 0.1 and 0.3 mg/kg. The mice were monitored daily and were

dx.doi.org/10.1021/bc400217g | Bioconjugate Chem. 2013, 24, 1256−1263

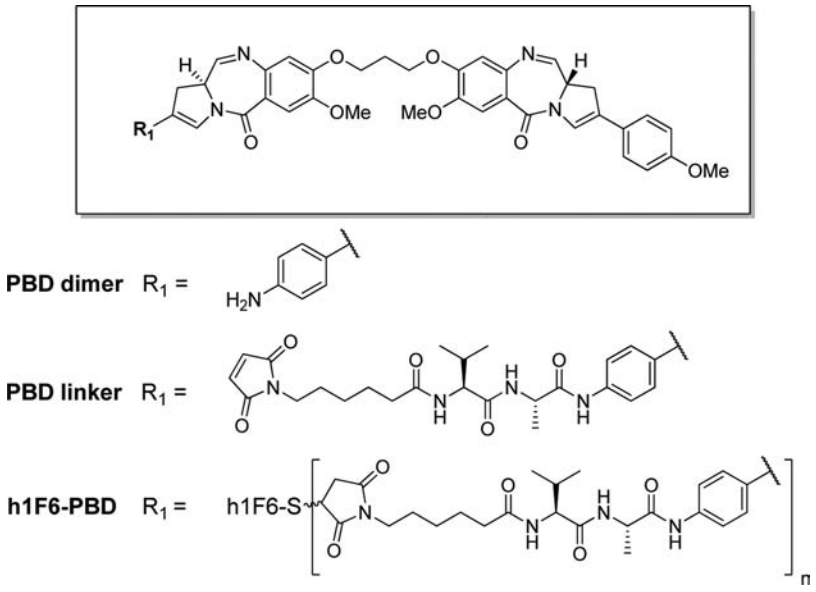

Figure 1. Structures of the PBD dimer, linker, and ADC.

terminated with symptoms of metastatic disease including hind limb paralysis, cranial swelling, bloated abdomen, scruffy coat, and hunched posture. Surviving mice were euthanized on day 100. Caki-1 and MHH-PREB-1 models: Caki-1 tumor fragments or MHH-PREB-1 cells (5×10^6) were implanted in the right flank of nude female mice or C.B-17 SCID mice, respectively. Mice were randomized to study groups (n = 5 for Caki-1, and n = 7 for MHH-PREB-1) on day 10 with each group averaging around 100 mm^3 tumor. The $h1F6_{239C}$-PBD and $hIgG_{239C}$-PBD ADCs were dosed ip according to a q7dx2 schedule at 0.1 and 0.3 mg/kg. Tumor volume as a function of time was determined using the formula $(L \times W^2)/2$. Animals were euthanized when tumor volume reached 1000 mm^3. Cured animals were euthanized on day 90 post implant.

ADC and Antibody ELISA Methods. Plasma samples from ADC-treated female BALB/c mice were analyzed for total $h1F6_{239C}$ (mAb) and total ADC (Drug) using two different types of ELISA methods. To measure mAb concentration, microtiter plates were coated with a commercially available murine mAb (2 μg/mL) that binds to the human kappa light chain region of the antibody component of the $h1F6_{239C}$-PBD. Standards, controls, and samples were then incubated on coated and blocked microtiter plates in duplicate after a 1/5 dilution into assay diluent (PTB buffer). Bound $h1F6_{239C}$-PBD was detected with biotinylated anti-ID-h1F6 mAb followed by addition of a polymer horseradish peroxidase conjugated to streptavidin (poly-HRP-SA). To measure PBD drug concentration (Drug), microtiter plates were coated with anti-ID-h1F6 mAb that binds to the variable region of the antibody component of the $h1F6_{239C}$-PBD antibody-drug conjugate (ADC). Standards, controls, and samples were then incubated on coated and blocked microtiter plates in duplicate after a 1/5 dilution into assay diluent (PTB buffer). Bound $h1F6_{239C}$-PBD was detected with a biotinylated anti-PBD mAb that binds to the PBD-linker portion of the ADC followed by addition of a polymer horseradish peroxidase conjugated to streptavidin (poly-HRP-SA). For both the mAb and drug ELISA methods, 3,3′,5,5′-tetramethylbenzidine (TMB) was used for detection which is converted from colorless TMB to a colored TMB derivative by horseradish peroxidase. The signal is proportional to the amount of $h1F6_{239C}$-PBD bound to the plate as measured by absorbance at OD450 nm-OD630 nm.

RESULTS

Drug-Linker Design and Synthesis. We focused on PBD dimers as a drug class for ADCs due to their potent cytotoxicity, broad anticancer activity, synthetic accessibility, and complementary mechanism to our lead auristatin-based platform technology.[1] PBD dimers cross-link DNA by binding in the minor groove and reacting with interstrand guanine residues at GATC or related sequences.[21−23] Published data with monomeric PBDs indicated that the most potent forms contain C-ring unsaturation and 2-aryl substituents.[24] Although not previously demonstrated, we reasoned that PBD dimers with a C-2 *para*-aniline residue would have high potency, and could be used for peptide linker attachment. The PBD dimer used here (Figure 1)[20] was prepared using established methods including a Suzuki coupling reaction to install the *para*-aniline residue.[24]

Much ADC research to date has focused on peptide-based linker strategies, both for auristatin[8,11] and other drug classes.[5−7] We have demonstrated that attaching a peptide linker directly to the drug via an aniline residue affords ADCs with favorable plasma stability and facile drug release within tumors.[7,11] For the PBDs, we employed the known protease-cleavable valine-alanine[5,6] sequence (Figure 1) that was known to be stable in circulation, but readily cleaved within target cells. Coupling of the maleimidocaproyl-valine-alanine acid to the aniline residue of the PBD dimer using the standard peptide coupling agent EEDQ allowed us to prepare the PBD-linker in a single step. The structure of the drug-linker is illustrated in Figure 1.

Conjugation of PBD-Linker to h1F6 and the $h1F6_{239C}$ mAbs. Our investigation of the PBD dimers as a drug class for ADCs began with the h1F6 antibody which targets the CD70 cancer antigen.[25] The expression of CD70 on both renal cell carcinoma (RCC) and non-Hodgkin lymphoma (NHL) (Table 1) is well documented,[26] and CD70 has limited normal tissue expression.[16] The antigen internalizes efficiently upon ADC binding.[25] Conjugation of the PBDs to mAbs required the use

Table 1. Cellular CD70 Antigen Expression, Rhodamine Efflux Ability, and in Vitro Cytotoxic Activity of the PBD Dimer and h1F6$_{239C}$-PBD ADC on Lymphoma and Renal Cell Carcinoma Lines

Cell Line	Antigens/cell (×10^3)	Rhodamine Efflux	Cytotoxic Activity IC_{50} (nM) PBD Dimer	h1F6$_{239C}$-PBD
Lymphoma				
Raji	23	Negative	0.4	0.8
MHH-PREB-1	28	Negative	1.0	0.4
WSU-DLCL2	35	Negative	0.1	0.6
KMH2	160	Unknown	0.15	0.05
Renal Cell Carcinoma				
786-O	190	Positive	0.3	0.1
UM-RC-3	70	Positive	0.5	0.2
ACHN	55	Negative	0.2	0.2
Caki-1	140	Negative	0.3	0.02

of significant amounts of cosolvents due to low aqueous solubility of the PBD-linker. We found that propylene glycol (50%) was an effective cosolvent that gave efficient conversion without precipitation of the drug-linker during the reaction and had no adverse effects on the protein.

Various constructs were investigated including 2- and 4-loaded ADCs on endogenous hinge cysteine residues of h1F6 and a site-specific 2-load ADC on h1F6$_{239C}$. For the hinge cysteine conjugates, the monoclonal antibody h1F6 was treated with tris(2-carboxyethyl)phosphine (TCEP) to partially reduce the interchain disulfide bonds and provide antibody with an average of 2 or 4 free thiols/antibody.[27] Conjugation of reduced h1F6 with 2 or 4 thiol groups/mAb with the PBD-linker resulted in ADCs having 13% and 45% aggregate, respectively (Table 2), as determined by size-exclusion

Table 2. Comparison of Aggregation and Unconjugated Antibody Percentages for 2- and 4-Loaded Hinge Cysteine Conjugates versus Engineered Cysteine Conjugates of the PBD Linker

	h1F6-PBD(4)	h1F6-PBD(2)	h1F6$_{239C}$-PBD
% Aggregate	45	13	1.6
% Unconjugated mAb	7.2	51	5.4

chromatography (Supporting Information Figure S1). Hydrophobic interaction chromatography of h1F6-PBD (average 2-load) indicated that approximately 50% of the mixture was unconjugated h1F6. Based on these results we concluded that the use of endogenous interchain disulfides for conjugation of this PBD-linker was not a viable approach for ADC formation.

In order to produce uniform ADCs with low aggregation levels, we used recombinant technologies to introduce new mAb cysteines for site-specific drug attachment. Cysteines were introduced at the 239 position on the mAb heavy chains, since this is a solvent accessible position[28] and was empirically proven to react with drug-maleimide derivatives. The h1F6$_{239C}$ construct was expressed in Chinese hamster ovary cells and was applied to the PBD-linker.

The process for conjugating the PBD-linker to h1F6$_{239C}$ is illustrated in Figure 2. The h1F6$_{239C}$ mAb, isolated from cell culture as cysteine disulfides, was treated with excess TCEP. This fully reduced both the position-239 cysteine disulfides and all interchain disulfide bonds. The mAb was then partially

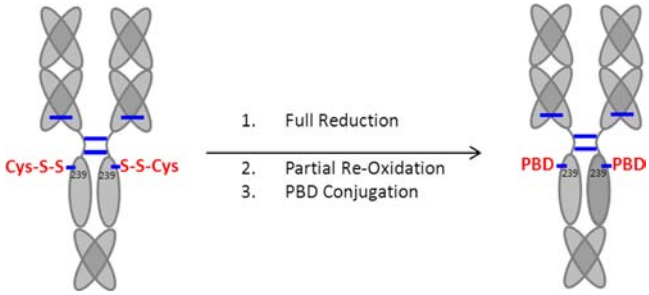

Figure 2. Conjugation process for the 239C antibody format. The engineered antibody, expressed in CHO cells, was isolated as the cysteine disulfide at position 239. The antibody was fully reduced with TCEP and partially reoxidized with dehydroascorbic acid. The resulting free cysteines at position 239 were conjugated to the PBD-linker to give the PBD ADC with nominally 2 drugs/mAb.

reoxidized with dehydroascorbic acid. Due to the proximity of the hinge cysteine residues, the reoxidation step selectively reformed the native disulfide bonds, but left the two engineered 239-cysteine residues in the reduced form and available for conjugation. Addition of the PBD-linker as a solution in propylene glycol resulted in efficient conjugation (1.9 drug/mAb) and PLRP-MS demonstrated exclusive loading of the PBD-linker onto the heavy chains of the antibody (Figure 3).

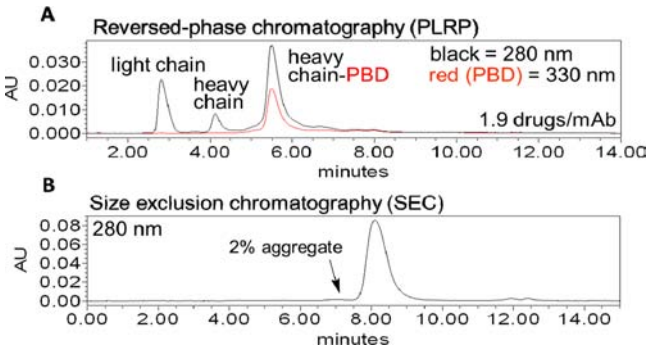

Figure 3. Analytical characterization of h1F6$_{239C}$-PBD. A. PLRP analysis of reduced ADC showed exclusive loading of PBD-linker on antibody heavy chain. B. Size exclusion analysis of h1F6$_{239C}$-PBD showed minimal aggregation.

Aggregation (1.6%) was significantly lower than that obtained by conjugating through endogenous hinge cysteines (Table 2). Thus, the recombinant construct provided superior ADCs compared to hinge disulfide conjugates in terms of ADC uniformity and aggregation levels.

Biological Evaluation of PBD Dimer and h1F6$_{239C}$-PBD. The initial in vitro evaluation of the PBD dimer small molecule established that the drug was highly potent on a panel of carcinoma and lymphoma cell lines including RCC (786-O, UM-RC-3, ACHN, and Caki-1), Hodgkin (KMH2), and NHL (Raji, MHH-PREB-1, WSU-DLCL2) (Table 1). The RCC lines, 786-O and UM-RC-3, are known to express the MDR-1 (P-glycoprotein) protein and efflux rhodamine dye,[29,30] yet potent activity was observed with the PBD dimer. The IC_{50} values ranged from 0.1 to 1.0 nM, consistent with the literature for this potent class of DNA-reactive agents.[17] Incorporation of the *para*-aniline residue onto one of the C-2 aryl groups did not lead to apparent loss in drug potency.

The cytotoxic activity of h1F6$_{239C}$-PBD was determined using the same panel of CD70-positive RCC and lymphoma

dx.doi.org/10.1021/bc400217g | *Bioconjugate Chem.* 2013, 24, 1256−1263

lines. Treatment was for 96 h, and IC_{50} values ranged between 0.2 and 0.8 nM ADC. These values are comparable to the free PBD dimer IC_{50} values and well below the antigen saturation concentration of 7 nM, or 1 μg/mL ADC. In addition, the effects were immunologically specific, as a nonbinding control ADC was ~1/1000th as potent as h1F6$_{239C}$-PBD (Figure 4).

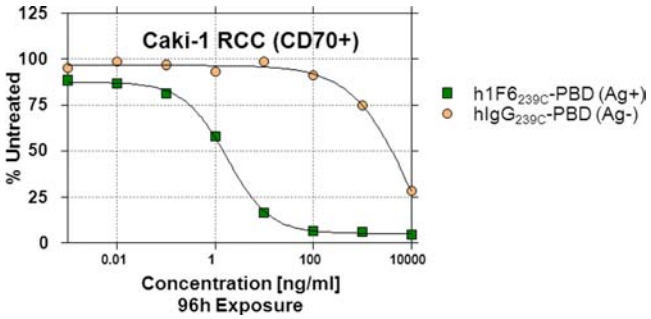

Figure 4. In vitro immunologic specificity of PBD ADCs on CD70-positive Caki-1 renal cell carcinoma line. Nonbinding hIgG$_{239C}$-PBD showed markedly reduced cytotoxic activity (~1000-fold) compared to h1F6$_{239C}$-PBD which binds the CD70 antigen.

We next turned our attention to evaluating the rodent toxicology, stability, pharmacokinetic (PK), and in vivo activities of the h1F6$_{239C}$-PBD conjugate. A single-dose toxicology study using BALB/c mice demonstrated that h1F6$_{239C}$-PBD was well tolerated at 2.5 mg/kg with no weight loss relative to untreated mice (data not shown). At a single 5 mg/kg dose, bone marrow toxicity occurred, which may be a clinically relevant finding.

As an initial evaluation of linker stability, we incubated the ADC in rat plasma for a period of 6 days and recovered the ADC using a resin that bound serum IgGs. Since no loss of drug from the ADC was found by PLRP analysis (Supporting Information Figure S2), we concluded that the linker was stable in plasma, and that no maleimide transfer to albumin took place during the observation period. Drug release could be achieved by treatment of a PBD ADC with the lysosomal protease cathepsin B, suggesting that this enzyme may be involved in the intracellular release of the active drug.

We then evaluated the PK of h1F6$_{239C}$-PBD in mouse using two different ELISA methods (Figure 5). The h1F6 component of the ADC in circulation was assessed using an antihuman IgG reagent, and conjugated PBD drug was measured using an antibody that recognized the PBD-linker component. In this experiment, the data for the ADC were compared to h1F6$_{239C}$ conjugated to *N*-ethylmaleimide (NEM). This allowed us to determine the impact the PBD-linker had on ADC clearance. Mice were injected with a single dose (0.3 or 1.0 mg/kg) of h1F6$_{239C}$-PBD or h1F6$_{239C}$-NEM, and blood samples were collected at set time points. We found a similar clearance profile for both the h1F6$_{239C}$-NEM and h1F6$_{239C}$-PBD. For example, at the 0.3 mg/kg dose, the half-lives were 14.0 and 12.3 days, respectively. The half-life of conjugated PBD, as determined by the antidrug ELISA, was 8.0 and 8.5 days when dosed at 1.0 and 0.3 mg/kg, respectively. The difference in the mAb ELISA and drug ELISA half-life measurements may be due to proteolytic loss of drug from the ADC, or to a modification of the conjugated PBD that is not recognized by the detection antibody.

In vivo activity studies were conducted in disseminated (ACHN RCC and Raji NHL) and subcutaneous (Caki-1 RCC and MHH-PREB-1 NHL) mouse xenografts (Figure 6). Each model was CD70-positive and the cell lines were sensitive to the h1F6$_{239C}$-PBD in vitro at sub-nM concentrations (Table 1). In vivo immunologic specificity was assessed by giving equivalent doses of the nonbinding control hIgG$_{239C}$-PBD. In the ACHN model, a cure rate of 100% (10/10 mice) was obtained with two weekly doses of 0.1 mg/kg of h1F6$_{239C}$-PBD. The effects were immunologically specific, since the nonbinding control group had no survivors at day 75 (Figure 6A). There was also a distinct survival advantage with immunological specificity demonstrated in the Raji lymphoma model (Figure 6B) with single doses of 0.1 and 0.3 mg/kg ADC. Using two weekly 0.3 mg/kg doses in nude mice bearing Caki-1 tumors resulted initially in 4/5 complete responses based on the absence of palpable tumor in these mice, with 3/5 cures at the end of the experiment (Figure 6C). The specificity controls had minimal effect. Finally, the MHH-PREB-1 NHL model in SCID mice was very sensitive to h1F6$_{239C}$-PBD with 100% cures (7/7 mice) with two weekly 0.1 mg/kg doses (Figure 6D), whereas the hIgG$_{239C}$-PBD control at the same dose was nearly devoid of activity. In all the models, h1F6$_{239C}$-PBD showed potent antitumor activities and high degrees of immunologic specificity at well-tolerated doses.

DISCUSSION

PBD dimers constitute a new drug class and cytotoxic mechanism for ADCs and complement the current technolo-

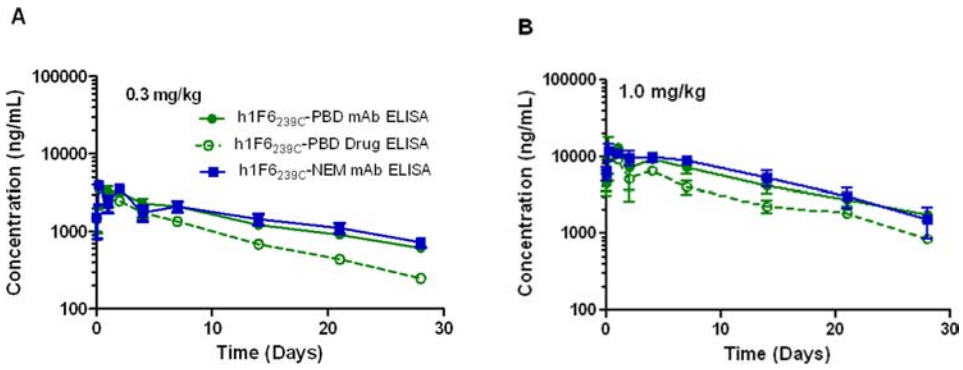

Figure 5. Pharmacokinetic measurements of h1F6$_{239C}$-PBD and h1F6$_{239C}$-NEM conjugates. A. Measurement of h1F6 antibody (mAb) and PBD drug (Drug) concentrations in mouse plasma after administration of a single 0.3 mg/kg dose of h1F6$_{239C}$-PBD or h1F$_{239C}$-NEM conjugate. B. Measurements of a single 1.0 mg/kg dose of h1F6$_{239C}$-PBD or h1F6$_{239C}$-NEM conjugate.

dx.doi.org/10.1021/bc400217g | *Bioconjugate Chem.* 2013, 24, 1256−1263

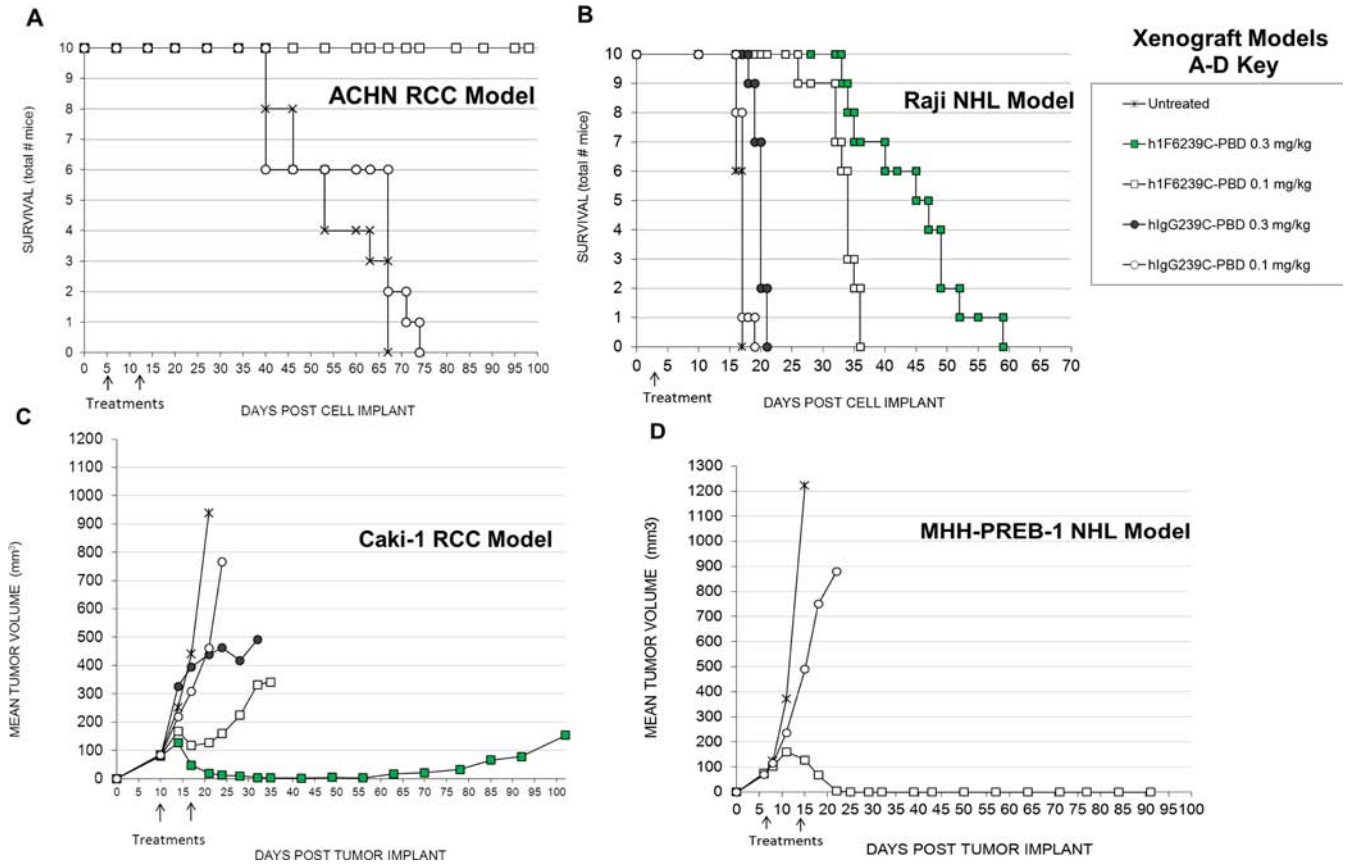

Figure 6. In vivo antitumor activity in xenograft models of RCC and NHL. A. ACHN, and B. Raji lymphoma disseminated models. Female SCID mice (n = 10) were injected intraperitoneally with ACHN cells (10^6) or intravenously Raji lymphoma cells (5×10^6). The h1F6$_{239C}$-PBD and hIgG$_{239C}$-PBD ADCs were dosed ip according to schedule at 0.1 or 0.3 mg/kg (arrows). The mice were monitored daily and were terminated with symptoms of metastatic disease. C. Caki-1, and D. MHH-PREB-1 subcutaneous models. Caki-1 tumor fragments or MHH-PREB-1 cells (5×10^6) were implanted in the right flank of female nude mice. Mice were randomized to study groups (n = 5 for Caki-1, and n = 7 for MHH-PREB-1) and treated when a 100 mm^3 tumor was reached. The h1F6$_{239C}$-PBD and hIgG$_{239C}$-PBD ADCs were dosed ip according to a q7dx2 schedule at 0.1 or 0.3 mg/kg (arrows). Tumor volume as a function of time was determined using the formula $(L \times W^2)/2$.

gies based on auristatin and maytansine antimitotic agents. They react with double-stranded DNA to form interchain DNA cross-links[21−23] that can elude common DNA repair mechanisms,[17] leading to potent cytotoxic activities. The highly potent PBD dimer used here is less sensitive to the P-glycoprotein resistance mechanism than other less potent ADC classes,[31] and other PBD analogs.[32,33] Both the PBD dimer free drug and conjugate were highly active against cancer cell lines that express P-glycoprotein and efflux rhodamine dye (Table 1). Since high P-glycoprotein expression is a significant negative prognostic indicator for RCC patients[34,35] as well as several other malignancies, a PBD ADC may have applications in settings where other drug classes are ineffective.

Standard conjugation methods, such as conjugation through antibody native hinge cysteine or lysine residues, afforded variably loaded species[36,37] which led to aggregation. In the case of the hydrophobic PBD-linker, conjugation via hinge cysteine residues failed to provide monomeric ADCs, and as a result, this method was abandoned. Site-specific conjugation to engineered cysteine residues, such as at position 239 of the antibody heavy chain, was vital for preparing PBD ADCs that were monomeric and well-defined. The site-specific introduction of cysteine residues for conjugation can offer other advantages such as high serum stability; however, stability does vary with mutation site.[38] In this example, when incubated in rat plasma for 6 days, essentially no drug loss from hIgG$_{239C}$-PBD was observed. This is comparable to data for one other engineered cysteine-based ADC, but superior to others.[39] The stability is higher than that shown for endogenous hinge cysteine conjugates.[12] The ADC and the NEM-modified mAb had the same PK profiles demonstrating a negligible impact on clearance by PBD-linker conjugation.

The activity of h1F6$_{239C}$-PBD reflects the potency of the PBD dimer, and is generally greater than ADCs employing other drug classes.[13,40] In the disseminated ACHN RCC and subcutaneous MHH-PREB-1 NHL xenografts, all of the mice were cured with two weekly 0.1 mg/kg doses of ADC. It is noteworthy that a 0.1 mg/kg dose of h1F6$_{239C}$-PBD carries 1 μg/kg of PBD dimer drug. By way of comparison, it is common for other classes to be dosed at 10- to 100-fold higher levels.[11,13,40] The treatment of solid tumors, in which exposure to the cytotoxic drug may be hampered by ADC penetration, could benefit with higher potency, as less drug would be required to have an antitumor effect.

With the approval of ADCETRIS (brentuximab vedotin) and KADCYLA (ado-trastuzumab emtansine), ADCs are emerging as effective therapies for treating cancer. The research presented here, in the context of an anti-CD70 therapy, represents several advances in ADC technology. These include a highly cytotoxic PBD dimer with a novel DNA-based

dx.doi.org/10.1021/bc400217g | Bioconjugate Chem. 2013, 24, 1256−1263

mechanism, a site-specific, well-defined conjugation method, stable conjugation chemistry, long circulating half-life, and broad and pronounced activity in mouse xenografts, including MDR-positive models, at well-tolerated doses. We expect that this technology will extend the scope of ADCs to include new cancer targets. While many important issues remain to be studied, including a detailed investigation of toxicology and the impact improved ADC stability has on tolerability and potency, the data presented here for h1F6$_{239C}$-PBD indicate that this new technology warrants further investigation for cancer therapy.[19]

■ ASSOCIATED CONTENT

Supporting Information

Size exclusion chromatograms and PLRP analysis. This material is available free of charge via the Internet at http://pubs.acs.org.

■ AUTHOR INFORMATION

Corresponding Author

*Tel. 425 527-4738. Fax. 425 527-4901. E-mail: sjeffrey@seagen.com.

Notes

The authors declare the following competing financial interest(s): With the exception of DET, all authors are employed by either Seattle Genetics, Inc., or Spirogen Ltd.

■ REFERENCES

(1) Senter, P. D., and Sievers, E. L. (2012) The discovery and development of brentuximab vedotin for use in relapsed Hodgkin lymphoma and systemic anaplastic large cell lymphoma. *Nat. Biotechnol. 30*, 631−7.

(2) Senter, P. D. (2009) Potent antibody drug conjugates for cancer therapy. *Curr. Opin. Chem. Biol. 13*, 235−44.

(3) Sievers, E. L., and Senter, P. D. (2013) Antibody-drug conjugates in cancer therapy. *Annu. Rev. Med. 64*, 15−29.

(4) Burke, P. J., Senter, P. D., Meyer, D. W., Miyamoto, J. B., Anderson, M., Toki, B. E., Manikumar, G., Wani, M. C., Kroll, D. J., and Jeffrey, S. C. (2009) Design, synthesis, and biological evaluation of antibody-drug conjugates comprised of potent camptothecin analogues. *Bioconjugate Chem. 20*, 1242−50.

(5) Burke, P. J., Toki, B. E., Meyer, D. W., Miyamoto, J. B., Kissler, K. M., Anderson, M., Senter, P. D., and Jeffrey, S. C. (2009) Novel immunoconjugates comprised of streptonigrin and 17-amino-geldanamycin attached via a dipeptide-p-aminobenzyl-amine linker system. *Bioorg. Med. Chem. Lett. 19*, 2650−3.

(6) Jeffrey, S. C., Nguyen, M. T., Andreyka, J. B., Meyer, D. L., Doronina, S. O., and Senter, P. D. (2006) Dipeptide-based highly potent doxorubicin antibody conjugates. *Bioorg. Med. Chem. Lett. 16*, 358−62.

(7) Jeffrey, S. C., Torgov, M. Y., Andreyka, J. B., Boddington, L., Cerveny, C. G., Denny, W. A., Gordon, K. A., Gustin, D., Haugen, J., Kline, T., Nguyen, M. T., and Senter, P. D. (2005) Design, synthesis, and in vitro evaluation of dipeptide-based antibody minor groove binder conjugates. *J. Med. Chem. 48*, 1344−58.

(8) Doronina, S. O., Bovee, T. D., Meyer, D. W., Miyamoto, J. B., Anderson, M. E., Morris-Tilden, C. A., and Senter, P. D. (2008) Novel peptide linkers for highly potent antibody-auristatin conjugate. *Bioconjugate Chem. 19*, 1960−3.

(9) Jeffrey, S. C., Andreyka, J. B., Bernhardt, S. X., Kissler, K. M., Kline, T., Lenox, J. S., Moser, R. F., Nguyen, M. T., Okeley, N. M., Stone, I. J., Zhang, X., and Senter, P. D. (2006) Development and properties of beta-glucuronide linkers for monoclonal antibody-drug conjugates. *Bioconjugate Chem. 17*, 831−40.

(10) Hamblett, K. J., Senter, P. D., Chace, D. F., Sun, M. M., Lenox, J., Cerveny, C. G., Kissler, K. M., Bernhardt, S. X., Kopcha, A. K., Zabinski, R. F., Meyer, D. L., and Francisco, J. A. (2004) Effects of drug loading on the antitumor activity of a monoclonal antibody drug conjugate. *Clin. Cancer. Res. 10*, 7063−70.

(11) Doronina, S. O., Toki, B. E., Torgov, M. Y., Mendelsohn, B. A., Cerveny, C. G., Chace, D. F., DeBlanc, R. L., Gearing, R. P., Bovee, T. D., Siegall, C. B., Francisco, J. A., Wahl, A. F., Meyer, D. L., and Senter, P. D. (2003) Development of potent monoclonal antibody auristatin conjugates for cancer therapy. *Nat. Biotechnol. 21*, 778−84.

(12) Alley, S. C., Benjamin, D. R., Jeffrey, S. C., Okeley, N. M., Meyer, D. L., Sanderson, R. J., and Senter, P. D. (2008) Contribution of linker stability to the activities of anticancer immunoconjugates. *Bioconjugate Chem. 19*, 759−65.

(13) Doronina, S. O., Mendelsohn, B. A., Bovee, T. D., Cerveny, C. G., Alley, S. C., Meyer, D. L., Oflazoglu, E., Toki, B. E., Sanderson, R. J., Zabinski, R. F., Wahl, A. F., and Senter, P. D. (2006) Enhanced activity of monomethylauristatin F through monoclonal antibody delivery: effects of linker technology on efficacy and toxicity. *Bioconjugate Chem. 17*, 114−24.

(14) Junutula, J. R., Flagella, K. M., Graham, R. A., Parsons, K. L., Ha, E., Raab, H., Bhakta, S., Nguyen, T., Dugger, D. L., Li, G., Mai, E., Lewis Phillips, G. D., Hiraragi, H., Fuji, R. N., Tibbitts, J., Vandlen, R., Spencer, S. D., Scheller, R. H., Polakis, P., and Sliwkowski, M. X. (2010) Engineered thio-trastuzumab-DM1 conjugate with an improved therapeutic index to target human epidermal growth factor receptor 2-positive breast cancer. *Clin. Cancer. Res. 16*, 4769−78.

(15) Grewal, I. S. (2008) CD70 as a therapeutic target in human malignancies. *Expert Opin. Ther. Targets 12*, 341−51.

(16) Boursalian, T. E., McEarchern, J. A., Law, C. L., and Grewal, I. S. (2009) Targeting CD70 for human therapeutic use. *Adv. Exp. Med. Biol. 647*, 108−19.

(17) Hartley, J. A., Hamaguchi, A., Coffils, M., Martin, C. R., Suggitt, M., Chen, Z., Gregson, S. J., Masterson, L. A., Tiberghien, A. C., Hartley, J. M., Pepper, C., Lin, T. T., Fegan, C., Thurston, D. E., and Howard, P. W. (2010) SG2285, a novel C2-aryl-substituted pyrrolobenzodiazepine dimer prodrug that cross-links DNA and exerts highly potent antitumor activity. *Cancer Res. 70*, 6849−58.

(18) Howard, P. W., Chen, Z., Gregson, S. J., Masterson, L. A., Tiberghien, A. C., Cooper, N., Fang, M., Coffils, M. J., Klee, S., Hartley, J. A., and Thurston, D. E. (2009) Synthesis of a novel C2/C2′-aryl-substituted pyrrolo[2,1-c][1,4]benzodiazepine dimer prodrug with improved water solubility and reduced DNA reaction rate. *Bioorg. Med. Chem. Lett. 19*, 6463−6.

(19) Sutherland, M. S., Walter, R. B., Jeffrey, S. C., Burke, P. J., Yu, C., Stone, I., Ryan, M. C., Sussman, D., Zeng, W., Harrington, K. H., Klussman, K., Westendorf, L., Meyer, D., Bernstein, I. D., Senter, P. D., Drachman, J. G., and McEarchern, J. A. (In Press) SGN-CD33A: A novel CD33-targeting antibody-drug conjugate utilizing a pyrrolobenzodiazepine dimer is active in models of drug-resistant AML.

(20) Howard, P. W., Gregson, S. J., Masterson, L. (2010) Unsymmetrical pyrrolobenzodiazepine-dimers for treatment of proliferative diseases. WO2010/43880 A1.

(21) Rahman, K. M., Thompson, A. S., James, C. H., Narayanaswamy, M., and Thurston, D. E. (2009) The pyrrolobenzodiazepine dimer SJG-136 forms sequence-dependent intrastrand DNA cross-links and monoalkylated adducts in addition to interstrand cross-links. *J. Am. Chem. Soc. 131*, 13756−66.

(22) Rahman, K. M., H., V., James, C. H., Howard, P. W., and Thurston, D. E. (2010) DNA sequence preference and adduct orientation of pyrrolo[2,1-c][1,4]benzodiazepine antitumor agents. *ACS Med. Chem. Lett. 1*, 427−32.

(23) Rahman, K. M., James, C. H., and Thurston, D. E. (2011) Effect of base sequence on the DNA cross-linking properties of pyrrolobenzodiazepine (PBD) dimers. *Nucleic Acids Res. 39*, 5800−12.

(24) Antonow, D., Kaliszczak, M., Kang, G. D., Coffils, M., Tiberghien, A. C., Cooper, N., Barata, T., Heidelberger, S., James, C. H., Zloh, M., Jenkins, T. C., Reszka, A. P., Neidle, S., Guichard, S. M., Jodrell, D. I., Hartley, J. A., Howard, P. W., and Thurston, D. E. (2010) Structure-activity relationships of monomeric C2-aryl pyrrolo[2,1-c][1,4]benzodiazepine (PBD) antitumor agents. *J. Med. Chem. 53*, 2927−41.

(25) Law, C. L., Gordon, K. A., Toki, B. E., Yamane, A. K., Hering, M. A., Cerveny, C. G., Petroziello, J. M., Ryan, M. C., Smith, L., Simon, R., Sauter, G., Oflazoglu, E., Doronina, S. O., Meyer, D. L., Francisco, J. A., Carter, P., Senter, P. D., Copland, J. A., Wood, C. G., and Wahl, A. F. (2006) Lymphocyte activation antigen CD70 expressed by renal cell carcinoma is a potential therapeutic target for anti-CD70 antibody-drug conjugates. *Cancer Res. 66*, 2328−37.

(26) McEarchern, J. A., Smith, L. M., McDonagh, C. F., Klussman, K., Gordon, K. A., Morris-Tilden, C. A., Duniho, S., Ryan, M., Boursalian, T. E., Carter, P. J., Grewal, I. S., and Law, C. L. (2008) Preclinical characterization of SGN-70, a humanized antibody directed against CD70. *Clin. Cancer. Res. 14*, 7763−72.

(27) Sun, M. M., Beam, K. S., Cerveny, C. G., Hamblett, K. J., Blackmore, R. S., Torgov, M. Y., Handley, F. G., Ihle, N. C., Senter, P. D., and Alley, S. C. (2005) Reduction-alkylation strategies for the modification of specific monoclonal antibody disulfides. *Bioconjugate Chem. 16*, 1282−90.

(28) Fraczkiewicz, R., and Braun, W. (1998) Exact and efficient analytical calculation of the accessible surface areas and their gradients for macromolecules. *J. Comput. Chem. 19*, 319−33.

(29) Lamy, T., Drenou, B., Grulois, I., Fardel, O., Jacquelinet, C., Goasguen, J., Dauriac, C., Amiot, L., Bernard, M., and Fauchet, R. (1995) Multi-drug resistance (MDR) activity in acute leukemia determined by rhodamine 123 efflux assay. *Leukemia 9*, 1549−55.

(30) Kawabata, M., Kobayashi, H., Mori, S., Sekiguchi, S., and Takemura, Y. (1997) Flow cytometric analysis of P-glycoprotein function by rhodamine 123 dye-efflux assay in human leukemia cells. *Rinsho Byori 45*, 891−8.

(31) Jawad, M., Seedhouse, C., Mony, U., Grundy, M., Russell, N. H., and Pallis, M. (2010) Analysis of factors that affect in vitro chemosensitivity of leukaemic stem and progenitor cells to gemtuzumab ozogamicin (Mylotarg) in acute myeloid leukaemia. *Leukemia 24*, 74−80.

(32) Aird, R. E., Thomson, M., Macpherson, J. S., Thurston, D. E., Jodrell, D. I., and Guichard, S. M. (2008) ABCB1 genetic polymorphism influences the pharmacology of the new pyrrolobenzodiazepine derivative SJG-136. *Pharmacogenomics J. 8*, 289−96.

(33) Guichard, S. M., Macpherson, J. S., Thurston, D. E., and Jodrell, D. I. (2005) Influence of P-glycoprotein expression on in vitro cytotoxicity and in vivo antitumour activity of the novel pyrrolobenzodiazepine dimer SJG-136. *Eur. J. Cancer 41*, 1811−8.

(34) Yu, D. S., Chang, S. Y., and Ma, C. P. (1998) The expression of MDR-1-related GP-170 and its correlation with anthracycline resistance in renal cell carcinoma cell lines and multidrug-resistant sublines. *Br. J. Urol. 82*, 544−7.

(35) Walsh, N., Larkin, A., Kennedy, S., Connolly, L., Ballot, J., Ooi, W., Gullo, G., Crown, J., Clynes, M., and O'Driscoll, L. (2009) Expression of multidrug resistance markers ABCB1 (MDR-1/P-gp) and ABCC1 (MRP-1) in renal cell carcinoma. *BMC Urol. 9*, 6.

(36) Lyon, R. P., Meyer, D. L., Setter, J. R., and Senter, P. D. (2012) Conjugation of anticancer drugs through endogenous monoclonal antibody cysteine residues. *Methods Enzymol. 502*, 123−38.

(37) Fleming, M. S., Zhang, W., Lambert, J. M., and Amphlett, G. (2005) A reversed-phase high-performance liquid chromatography method for analysis of monoclonal antibody-maytansinoid immunoconjugates. *Anal. Biochem. 340*, 272−8.

(38) Shen, B. Q., Xu, K., Liu, L., Raab, H., Bhakta, S., Kenrick, M., Parsons-Reponte, K. L., Tien, J., Yu, S. F., Mai, E., Li, D., Tibbitts, J., Baudys, J., Saad, O. M., Scales, S. J., McDonald, P. J., Hass, P. E., Eigenbrot, C., Nguyen, T., Solis, W. A., Fuji, R. N., Flagella, K. M., Patel, D., Spencer, S. D., Khawli, L. A., Ebens, A., Wong, W. L., Vandlen, R., Kaur, S., Sliwkowski, M. X., Scheller, R. H., Polakis, P., and Junutula, J. R. (2012) Conjugation site modulates the in vivo stability and therapeutic activity of antibody-drug conjugates. *Nat. Biotechnol. 30*, 184−9.

(39) Junutula, J. R., Raab, H., Clark, S., Bhakta, S., Leipold, D. D., Weir, S., Chen, Y., Simpson, M., Tsai, S. P., Dennis, M. S., Lu, Y., Meng, Y. G., Ng, C., Yang, J., Lee, C. C., Duenas, E., Gorrell, J., Katta, V., Kim, A., McDorman, K., Flagella, K., Venook, R., Ross, S., Spencer, S. D., Lee Wong, W., Lowman, H. B., Vandlen, R., Sliwkowski, M. X., Scheller, R. H., Polakis, P., and Mallet, W. (2008) Site-specific conjugation of a cytotoxic drug to an antibody improves the therapeutic index. *Nat. Biotechnol. 26*, 925−32.

(40) Tassone, P., Gozzini, A., Goldmacher, V., Shammas, M. A., Whiteman, K. R., Carrasco, D. R., Li, C., Allam, C. K., Venuta, S., Anderson, K. C., and Munshi, N. C. (2004) In vitro and in vivo activity of the maytansinoid immunoconjugate huN901-N2′-deacetyl-N2′-(3-mercapto-1-oxopropyl)-maytansine against CD56+ multiple myeloma cells. *Cancer Res. 64*, 4629−36.